Published in final edited form as:

Hepatology. 2018 September ; 68(3): 1111–1124. doi:10.1002/hep.29902.

Loss of PDK4 switches the hepatic NF-κB/TNF pathway from pro-survival to pro-apoptosis

Jianguo Wu[1,*], **Yulan Zhao**[1], **Young-Ki Park**[2], **Ji-Young Lee**[2], **Ling Gao**[3,4,5], **Jiajun Zhao**[3,4,5], **Li Wang**[1,6,7]

[1]Department of Physiology and Neurobiology, Institute for Systems Genomics, University of Connecticut, Storrs, CT 06269

[2]Department of Nutritional Sciences, Institute for Systems Genomics, University of Connecticut, Storrs, CT 06269

[3]Department of Endocrinology, Shandong Provincial Hospital affiliated to Shandong University, Jinan, Shandong, 250021, China

[4]Shandong Clinical Medical Center of Endocrinology and Metabolism, Jinan, Shandong, 250021, China

[5]Institute of Endocrinology and metabolism, Shandong Academy of Clinical Medicine, Jinan, Shandong, 250021, China

[6]Veterans Affairs Connecticut Healthcare System, West Haven, CT 06516

[7]Department of Internal Medicine, Section of Digestive Diseases, Yale University, New Haven, CT 06520

Abstract

It has been established that NF-κB members promote survival by upregulating anti-apoptotic genes and that genetic and pharmacological inhibition of NF-κB is required for TNF-induced hepatocyte apoptosis. In this study, we demonstrate that this pro-survival pathway is switched to pro-apoptosis under pyruvate dehydrogenase kinase 4 (PDK4)-deficient conditions. PDK4-deficiency triggered hepatic apoptosis concomitantly with increased numbers of aberrant mitochondria, ROS production, sustained JNK activation, and reduction of GSH. Interestingly, PDK4 retained p65 in cytoplasm via a direct protein-protein interaction. Disruption of PDK4-p65 association promoted p65 nuclear translocation. This in turn facilitated p65 binding to the TNF promoter to activate TNF-TNFR1 apoptotic pathway. *Pdk4*$^{-/-}$ livers were sensitized to Jo2 and

[*]*Corresponding author:* Jianguo Wu (jianguo.wu@uconn.edu), 75 North Eagleville Rd., U3156, Storrs, CT 06269. Tel: 860-486-0857; Fax: 860-486-3303.

Conflict of Interest

The authors declare that they have no conflict of interest.

Author Contributions

J.W. designed and performed experiments and prepared the manuscript. Y.Z. performed experiments and provided technical support. L.G. and J.Z. provided technical support. Y.P. and J.L. assisted with Seahorse experiment. L.W. supervised the work and wrote the manuscript.

Supporting Material

Supporting material for this article includes 12 Supporting figures, one word document containing detailed experimental procedures and a primer table.

GalN/LPS-mediated apoptotic injury which was prevented by the inhibition of p65 or TNFR1. The pro-survival activity of TNF was shifted, which was switched to a pro-apoptotic activity in *Pdk4*$^{-/-}$ hepatocytes as a result of impaired activation of pro-survival NF-κB targets. *Conclusion:* PDK4 is indispensible to dictate the fate of TNF/NF-κB-mediated hepatocyte apoptosis.

Keywords

Hepatocytes; Cell death; Mitochondria; Liver injury; PDK4

Introduction

Pyruvate dehydrogenase kinase 4 (PDK4) acts to inactivate the pyruvate dehydrogenase complex (PDC) by phosphorylating the pyruvate dehydrogenase (PDH), thereby dictating the conversion of acetyl-coenzyme A (Acetyl-CoA) from pyruvate.(1) The primary research focus in the past decade has been on PDK4-related metabolic functions;(2) however, emerging evidence suggests a pleotropic role of PDK4 in promoting tumorigenesis.(3) A recent report reveals that PDK4 activates SMAD1/5/8 by phosphorylation and is dual-localized in the cytosol and mitochondria.(4) Investigating PDK4's non-canonical function and its crosstalk with cytosol molecules would greatly expand the understanding of its regulatory roles in human diseases.

The two apoptotic pathways are the intrinsic mitochondrion-dependent pathway and the extrinsic apoptosis pathway.(5) The intrinsic pathway can be activated by DNA damaging agents, stress, hypoxia, and reactive oxygen species (ROS). The extrinsic pathway is at least in part mediated by tumor necrosis factor (TNF) binding to its receptors. TNF receptor activation leads to recruitment of different adaptor proteins. These death adaptors in turn couple with cell death effectors (e.g. pro-caspase-8 and pro-caspase-10), form the death-inducing signaling complex (DISC) and generate an apoptotic signaling cascade initiated by the cleavage and activation of caspases.(6)

NF-κB family of transcription factors exist as a homo- or heterodimer consisting of various combinations of its family members. In resting cells, NF-κB proteins reside in the cytoplasm in an inactive form, bound by members of the inhibitory IκB family. For the canonical (classical) NF-κB pathway, the activating signaling molecules, including TNF and interleukin-1 β (IL-1β), can be mediated through the tumor necrosis factor receptor (TNFR) and interleukin-1 receptor (IL-1R), respectively. These trigger p65/p50 nuclear translocation and binding to target gene promoters.(7) The NF-κB signaling pathway is particularly relevant to liver diseases including hepatitis, liver fibrosis, and hepatocellular carcinoma (HCC).(8)

The intriguing interplay between NF-κB and TNF has been implicated in hepatocytes. TNF elicits distinct responses by positively modulating liver regeneration(9) and inducing cell death during hepatotoxic injury.(10) Interestingly, NF-κB inhibition converts the effect of TNF response from proliferation to apoptosis in a hepatocyte cell line.(11) Although it is well known that NF-κB is a family of cell survival transcription factors by upregulating anti-apoptotic genes, the role of NF-κB as a double-edged sword in mouse hepatocytes injury

and HCC development has been reported.(8, 12) New signaling molecules to convey the crosstalk between NF-κB and TNF remain to be uncovered.

PDK4 expression was downregulated in human HCC specimens and several key cell cycle regulators were upregulated in livers of *Pdk4*$^{-/-}$ mice.(13) Because cell proliferation and apoptosis are the opposite processes to control a cell fate, we aimed at understanding the role of PDK4 in cellular apoptosis in this study. Unexpectedly, we discovered an essential role of PDK4 as a checkpoint to dictate the fate of hepatocyte apoptosis by mediating the crosstalk between NF-κB and TNF.

Materials and Methods

Wild-type (WT) and *Pdk4*$^{-/-}$ mice (13) were handled in accordance with a protocol approved by the Institutional Animal Care and Use Committee (IACUC) at the University of Connecticut. All mice were of C57BL/6J (inbred strain) genetic background and were housed under the same conditions at the UConn animal facility. The detailed breeding information about WT and *Pdk4*$^{-/-}$ mice was provided in the Supporting Information. Anti-Mouse CD95 (Jo2) (#554255; BD Pharmingen) was diluted in PBS. Two-month-old male mice were intravenously (tail) injected with plasmids (50 μg per mouse) using TurboFect *in vivo* Transfection reagent (#R0541; Thermo Fisher Scientific). Three days after injection, mice were injected intraperitoneally (i.p.) with Jo2 and sacrificed at different time points.(5) We used an established D-(+)-Galactosamine (GalN)/LPS apoptotic injury model.(14) Primary hepatocytes isolation and culture, liver histology, Western blot, immunofluorescence and terminal deoxynucleotidyl transferase dUTP nick end labeling (TUNEL) staining were described previously.(15–19) Flow cytometry, Co-immunoprecipitation (Co-IP), GST pull-down, Chromatin immunoprecipitation-Quantitative PCR (CHIP-qPCR), qPCR, and luciferase reporter assay were reported previously.(20–26)

For additional and detailed experimental procedures and statistical analysis please refer to Supporting Information.

Results

Knockdown of PDK4 in HCC cells decreased cell viability by inducing apoptosis

We generated *in vitro* HCC cell models with PDK4 knockdown. The PDK4 mRNA and protein were reduced by two shRNAs (shPDK4 #1 and #2) in Huh7 and Hep3B cells with a similar knockdown efficacy (Supporting Fig. 1). Following PDK4 knockdown, cell viability (steady-state cell number) was evaluated for 6 days by MTS assay, which revealed noticeably lower cell numbers in shPDK4 #1 and #2 cells vs shCTL cells (Fig. 1A). Foci formation assay revealed that loss of PDK4 drastically inhibited Huh7 and Hep3B cells formation of colonies (Fig. 1B).

PARP protein cleavage is a marker of activated apoptosis. No cleaved PARP proteins were detected in shCTL cells, however they were strikingly induced in shPDK4 cells (Fig. 1C). Caspases are the central components of apoptotic response. The activities of effector caspase-3, as well as the initiator caspases-8 and -9, were all induced in shPDK4 cells (Fig.

1D), suggesting that both extrinsic and intrinsic pathways were activated. Caspase-3 inhibitor and pan-caspase inhibitor completely blocked shPDK4-induced apoptosis, while caspase-8 inhibitor and caspase-9 inhibitor partially rescued it (Supporting Fig. 2A–C). We determined the apoptotic rate using flow cytometry. In comparison with shCTL Huh7 or Hep3B cells, the early apoptotic (Annexin V-FITC + /PI −, lower right quadrant of each plot) and late apoptotic/necrotic (Annexin V-FITC + /PI +, upper right quadrant of each plot) cells were markedly increased in shPDK4 cells (Fig. 1E). Taken together, the results demonstrated that loss of PDK4 function induced cellular apoptosis.

Knockdown of PDK4 in HCC cells disrupted mitochondrial function and respiration

A diagram elucidated when various assays were performed in shPDK4 cells (Supporting Fig. 3A). Although massive apoptosis occurred during the 1st week of PDK4 knockdown, some cells survived despite maintaining ~50% PDK4-depletion (Supporting Fig. 3B). Because shPDK4 #1 and #2 in Huh7 and Hep3B cells produced similar apoptotic phenotype (Fig. 1), shPDK4 #2 Huh7 cells were used for further analysis.

Transmission electron microscope (TEM) revealed that shPDK4 cells displayed chromatin fragmentation and condensation (Fig. 1F-a, blue arrows), a characteristic morphologic manifestation of apoptosis. TEM also revealed increased mitochondria number in shPDK4 vs shCTL cells. Some mitochondria in shPDK4 cells lost clear edges (yellow arrows), whereas others showed enlarged cavities as vacuoles (green arrows). In addition, the mitochondrial cristae was distorted and swollen (red arrowheads) in shPDK4 cells compared with control cells. In addition, one-year-old *Pdk4*$^{-/-}$ hepatocytes were enriched with lipid droplets and displayed enlarged endoplasmic reticulum (ER) cavity and increased lysosome number (Supporting Fig. 4A and B).

The Seahorse assay (Supporting Fig. 5) was used to determine mitochondria respiration. The basal respiration, maximal respiration, spare respiratory capacity, and the percentage of spare respiratory capacity were all significantly increased in shPDK4 vs shCTL cells (Fig. 1F-b, Supporting Fig. 6A). Interestingly, mitochondrial membrane potential ($\Delta\psi m$) was decreased in apoptotic cells, but was maintained, even with moderate increasing, in surviving cells (Supporting Fig. 7A). The expression of mitochondria biogenesis regulator PGC1α was not altered in shPDK4 cells (Supporting Fig. 7B). However, the cellular reactive oxygen species (ROS) levels were highly increased in shPDK4 vs shCTL cells (Fig. 1F-c), demonstrating that PDK4 knockdown led to oxidative stress. Corresponding to potentiated ROS production, we examined five electron leakage sites based on mitochondrial superoxide/H_2O_2 production in Amplex UltraRed Assay and found that the sites III_{Qo} and mitochondrial glycerol-3-phosphate dehydrogenase (mGPDH) were disturbed with more electron leakages in shPDK4 cells comparing with shCTL cells (Supporting Fig. 7C).

We further measured cellular PDH activities in shCTL and shPDK4 cells cultured under normal (N) or low (L) glucose concentrations (Fig. 1F-d). In shCTL cells, low glucose increased PDH activity, which may be a compensatory response. However, PDH activity remained at constant high levels in shPDK4 cells. The higher PDH activity rendered by down-regulation of PDK4 corresponded to the lower NAD/NADH ratio (Supporting Fig.

6B), suggesting enhanced NADH production. Collectively, the results suggested that loss of PDK4 function in HCC cells disrupted mitochondria function and induced apoptosis.

Diminishing PDK4 expression activated TNF pathway by inducing NF-κB nuclear translocation

To define the cell signaling pathways leading to apoptosis after PDK4 knockdown, 84 key genes from cell death pathways (including apoptosis, autophagy and necrosis) were simultaneously assayed using the RT^2 Profiler PCR array in Huh7 and Hep3B cells transfected with shCTL and shPDK4, respectively (Supporting Fig. 8). As expected, a differential gene expression pattern was observed in Huh7 and Hep3B cells due to their different genetic background. Interestingly, TNF, baculoviral IAP repeat-containing protein 3 (BIRC3, also named c-IAP2), and coiled-coil domain-containing protein 103 (CCDC103) were found commonly upregulated in shPDK4 Huh7 and Hep3B cells (Fig. 2A) with TNF showing the highest elevation (125 fold in Huh7 and 64 fold in Hep3B). The induction of *TNF, BIRC3* and *CCDC103* mRNA in shPDK4 cells was validated by qPCR (Fig. 2B). ELISA also detected increased TNF protein in cell culture supernatants (secreted form) and in cell lysates (cellular form) in shPDK4 cells (Fig. 2C). Notably, the cellular form of TNF was more highly induced than the secreted form.

Given that BIRC3 and TNF, both of which are NF-κB target genes,(27) were upregulated in shPDK4 cells, we examined the activity of NF-κB pathway mediated by p65 nuclear translocation. The p65 protein was highly enriched in the nuclear fraction of shPDK4 vs shCTL cells (Fig. 2D). Immunofluorescence staining further revealed an enhanced p65 nuclear translocation in shPDK4 cells (Fig. 2E). We next performed ChIP assay using sheared chromatin (Supporting Fig. 9A), which detected a marked increase of p65 occupancy in *TNF* and *BIRC3* promoters (Fig. 2F, Supporting Fig. 9B). Interestingly, the *CCDC103* gene promoter was also bound by significant amount of p65, suggesting *CCDC103* as a new target of the canonical NF-κB signaling. Further, the p65 occupancy on the promoter of *c-FLIP*, a well-known target of NF-κB, was also increased (Supporting Fig. 9C). Taken together, the results demonstrated that diminishing PDK4 expression resulted in activation of the NF-κB/TNF signaling pathway.

PDK4 interacted with NF-κB/p65 to regulate canonical NF-κB signaling

To gain molecular insights into the function of PDK4 in NF-κB signaling, we determined whether PDK4 was associated with p65. Confocal imagining of the subcellular localization of PDK4 and p65 in Huh7 cells revealed a co-localization of both proteins in cytoplasm, which was partially overlapped with the mitochondria marker Mito-red (Fig. 3A). Co-Immunoprecipitation (Co-IP) identified an interaction of PDK4 with p65 but not with the PCNA protein in Huh7 cells (Fig. 3B, left). The endogenous interaction between PDK4 and p65 was also observed in both cytosolic and mitochondrial compartments but not in nuclear extracts in Hepa1 cells (Fig. 3B, right). GST pulldown assay further confirmed a direct physical interaction between p65 protein and GST-PDK4 fusion protein (Fig. 3C). Thus, PDK4 protein bound to the NF-κB p65 subunit.

Next, we asked whether PDK4 functionally responded to NF-κB activation. Given that loss of PDK4 induced cellular ROS accumulation (Fig. 1F-c), we stimulated Huh7 cells with H_2O_2 or deprivation of nutrients; both were reported to activate canonical NF-κB signaling in other model systems.(28, 29) H_2O_2 treatment (24 hr) resulted in a significant dissociation between PDK4 and p65 protein (Fig. 3D, left). When cells were deprived of glucose for 48 hr, the interaction of PDK4 and p65 was also impaired (Fig. 3D, right). Deprivation of glutamine showed a minimal effect. Thus, knockdown of PDK4 resulted in increased ROS production, which in turn further disrupted the PDK4 and p65 protein interaction. Such event released p65 to facilitate its nuclear translocation. To further identify the NF-κB subunits that mediate NF-κB activation in the absence of PDK4, we performed immunoprecipitation in shPDK4 Huh7 cells. p65 interacted with RELB, C-Rel, p50 and p52, and p65-p50 and p65-RELB interactions were potentiated under PDK4 knockdown condition (Supporting Fig. 9D). The Re-CHIP assay revealed that p65 co-occupied *TNF* promoter predominantly with p50, and to a less extent with RELB and C-Rel (Supporting Fig. 9E). These results indicated that p50 served as the primary binding partner of p65 in the absence of PDK4.

Considering TNF and lipopolysaccharide (LPS) as potent NF-κB signaling activators, we examined the crosstalk between PDK4 and TNF/LPS in regulating the NF-κB signaling. Overexpression of PDK4 did not alter basal p65 activity but markedly attenuated its stimulation by TNF and LPS in Huh 7 cells (Fig. 3E), suggesting PDK4 was able to sequester NF-κB. We constructed *TNF, BIRC3* and *CCDC103* promoter luciferase reporters, all of which contain the NF-κB/p65 binding site (Supporting Fig. 10A). As expected, the promoters of *TNF, BIRC3* and *CCDC103* were activated by p65 overexpression, which were suppressed by co-expressing PDK4 in a dose dependent manner (Fig. 3F). Single NF-κB site mutation partially decreased p65-mediated *TNF, BIRC3* and *CCDC103* promoter activities (Supporting Fig. 10B) whereas mutation of all sites completely blocked p65 transactivation (Fig. 3F). Taken together, the results suggested that PDK4 functionally restrained the activation of NF-κB signaling.

Inhibition of NF-κB/TNF signaling prevented shPDK4-induced apoptosis

Since *BIRC3* encodes a member of the IAP (Inhibitor of Apoptosis) family of proteins that inhibit apoptosis,(30) whereas *CCDC103* is a dynein arm attachment factor involved in necrotic cell death response,(31) we hypothesized that the induction of TNF in shPDK4 cells may play a major role in PDK4-mediated cell death, considering its established pro-apoptotic function.(32)

To test this hypothesis, we generated shPDK4 Huh7 cells with simultaneous knockdown of TNF receptors (TNFR1, TNFR2), BIRC3, or CCDC103 (Fig. 4A). TNFR1 is ubiquitously expressed whereas TNFR2 is mainly expressed in immune cells.(6) Consistently, we found that TNFR1, but not TNFR2, was expressed in Huh7 cells (Fig. 4A). Loss of TNFR1 largely prevented apoptotic cell death in shPDK4 cells, whereas knockdown of BIRC3 and CCDC103 had no major effect (Fig. 4B). Similarly, ablation of NF-κB activation by knocking down p65 (Fig. 4C) significantly impaired shPDK4-induced apoptosis (Fig. 4D).

Therefore, our loss of function studies demonstrated that the activation of NF-κB/TNF signaling was responsible for shPDK4-induced apoptosis in HCC cells.

Pdk4$^{-/-}$ hepatocytes were susceptible to oxidative insult and apoptosis inducers

To illustrate whether *Pdk4*-deficient hepatocytes are susceptible to apoptosis, we isolated primary hepatocytes from WT and *Pdk4*$^{-/-}$ mice and treated the cells with H2O2 (intrinsic pathway inducer) and TNF (extrinsic pathway inducer). *Pdk4*$^{-/-}$ hepatocytes were more sensitive to H2O2 with respect to cell viability, as the cells showed significantly lower IC50 (H2O2: *Pdk4*$^{-/-}$ 162.5 μM vs WT 294.3 μM) (Fig. 4E). Similarly, when hepatocytes were challenged with cycloheximide (CHX) to sensitize TNF's efficacy, *Pdk4*$^{-/-}$ hepatocytes were more susceptible to TNF (IC50: *Pdk4*$^{-/-}$ 10.9 ng/ml vs WT 24.4 ng/ml). These were accompanied by the increased caspase-3, -8 and -9 activities in *Pdk4*$^{-/-}$ vs WT hepatocytes (Fig. 4F). Therefore, loss of PDK4 function sensitized hepatocytes to apoptotic stimuli.

Ectopic expression of PDK4 protected liver from Jo2-induced apoptosis by restraining NF-κB/TNF activation

To elucidate the contribution of PDK4 in regulating apoptosis *in vivo*, we used an acute liver injury model, Fas (CD95)-mediated liver apoptosis.(33) WT mice of 8-week-old were i.v. injected with empty vector (EV) or PDK4 overexpression plasmid. After 3 days, PDK4 overexpression in mouse liver was validated by Western blot (Fig. 5A-a). Mice were then i.p. injected with an anti-Fas agonistic antibody Jo2 (10 μg/mouse). Six hr post Jo2 administration, EV livers became macroscopically hemorrhagic and swollen, whereas PDK4 livers showed significant protection (Fig. 5A-b). H&E staining revealed that Jo2 treatment led to extensive red blood cell infiltration in EV livers, which was to a much less extent in PDK4 overexpressed livers (Fig. 5A-c). The Jo2 antibody showed lethal effect in WT mice. (33) PDK4 overexpression significantly increased the viability of mice challenged with Jo2 (Fig. 5A-d). The plasma ALT levels were also alleviated in PDK4 overexpressed mice (Supporting Fig. 11), suggesting a protective effect. TUNEL staining further revealed decreased hepatic apoptosis in PDK4 vs EV mice (Fig. 5B-a). Consistently, caspase-3 activation (Fig. 5B-b), PARP and BID cleavage, and Cytochrome C and Smac/DIABLO release (Fig. 5B-c) were markedly diminished by PDK4 overexpression comparing with EV mice, which was accompanied by the alleviated ROS production (Fig. 5C). Because ROS acts as a potent NF-κB activator,(34) we examined NF-κB/p65 nuclear translocation in Jo2-treated EV and PDK4 livers. Jo2 induced p65 nuclear protein as well as its activity in EV livers, which were significantly decreased in PDK4 livers (Fig. 5D). Consistently, Jo2-induced TNF levels were largely reduced by PDK4 overexpression (Fig. 5E). Taken together, the results demonstrated that ectopic expression of PDK4 protected liver from Jo2-induced apoptosis by impeding NF-κB/p65-TNF activation.

Knockdown of p65 and TNFR1 alleviated hepatic apoptosis in Pdk4$^{-/-}$ mice

To determine the direct effect of NF-κB/p65-TNF signaling in PDK4-mediated apoptosis, loss-of-function rescue studies were performed in *Pdk4*$^{-/-}$ mice with liver specific knockdown of p65 or TNFR1 (Fig. 5F-a). Mice were i.v. injected with control, shp65, or shTNFR1 plasmids for 3 days, followed by administrating with a reduced dose of Jo2 (5 μg/kg body weight) for 6 hr to mitigate its toxicity. Both shp65 and shTNFR1 reduced Jo2-

induced PARP protein cleavage (Fig. 5F-a). As revealed by TUNEL staining, Jo2 caused more severe apoptosis in *Pdk4*$^{-/-}$ vs WT livers and *in vivo* knockdown of p65 or TNFR1 in *Pdk4*$^{-/-}$ mice significantly alleviated hepatic sensitivity to Jo2 (Fig. 5F-b). The hepatic caspase-3 activation was similarly diminished by knockdown of either p65 or TNFR1 in *Pdk4*$^{-/-}$ mice livers (Fig. 5F-c).

Pdk4-deficiency facilitated whereas overexpression of PDK4 protected liver against GalN/LPS-induced apoptotic injury

D-galactosamine (GalN)/LPS administration induces apoptotic liver injury specifically confined to hepatocytes,(18) which was applied to WT, *Pdk4*$^{-/-}$ and PDK4 overexpression (PDK4) mice. Gross liver morphology (Fig. 6A-a) and H&E staining (Fig. 6A-b) revealed aggravated liver injury induced by GalN/LPS in *Pdk4*$^{-/-}$, which was protected in PDK4 mice. The severity of injury in *Pdk4*$^{-/-}$ livers corresponded to short survival time (Fig. 6A-c), high serum ALT levels (Fig. 6B) and increased caspase-3 cleavage (Fig. 6C). In addition, increased hepatic NF-κB/p65 activity and enhanced TNF and ROS production (Fig. 6D-a, -b, -c, -d), decreased hepatic GSH levels and sustained JNK/c-Jun activation (Fig. 6E-a, -b) were observed in *Pdk4*$^{-/-}$ mice. Remarkably, these changes were reversed in PDK4 mice. Furthermore, knockdown of p65 and TNFR1 in *Pdk4*$^{-/-}$ livers decreased GalN/LPS-induced apoptosis (Fig. 6F-a) which correlated with the reduced TNF levels (Fig. 6F-b).

Pdk4-deficiency shifted pro-survival function of NF-κB to apoptosis

It is well established that NF-κB has strong pro-survival effects through activating pro-survival genes.(23) We conducted additional experiments to address this paradox, given that NF-κB was activated however apoptotic death occurred in *Pdk4*-deficient cells. We first analyzed the expression of pro-apoptotic proteins in the presence of TNF stimulation. TNF alone induced caspase-3 activation, PARP and BID cleavage, and Cytochrome C and Smac/DIABLO release in *Pdk4*$^{-/-}$, but not in WT primary hepatocytes (Fig. 7A, left). Similar results were observed in shPDK4 vs shCTL cells (Fig. 7A, right). TNF stimulation also aggravated the apoptosis in shPDK cells. When TNF was combined with cycloheximide (CHX), a protein translation inhibitor sensitizing cells to TNF-induced apoptosis, pro-apoptotic proteins were induced or cleaved in WT hepatocytes, but to a stronger extent in *Pdk4*$^{-/-}$ hepatocytes (Fig. 7A, middle). In contrast, TNF-induced the expression of several pro-survival proteins including A20, c-IAPs and c-FLIP, in WT hepatocytes and shCTL cells (Fig. 7B), whereas such effect was largely impaired in *Pdk4*$^{-/-}$ hepatocytes and shPDK4 cells. At the mRNA levels, the activation of pro-survival targets of NF-κB by TNF was also impaired under *Pdk4*-deficient conditions (Supporting Fig. 12). Consistent with the *in vivo* results (Fig. 6E), a sustained JNK activation was observed in *Pdk4*$^{-/-}$ hepatocytes and shPDK4 HCC cells (Fig. 7C). On the other hand, reduced GSH levels were observed in PDK4-deficient cells (Fig. 7D).

Discussion

As a metabolic switch of glucose oxidation and TCA cycle, the role of PDK4 beyond metabolism remains elusive. In this study, we reveal that PDK4 is essential for TNF to

execute its pro-survival function via NF-κB and that *Pdk4*-deficiency shifts this anti-apoptosis pathway toward pro-apoptosis (Fig. 8).

We show that depletion of PDK4 in HCC cells induces spontaneous apoptotic cell death, which is accompanied by the disruption of mitochondria morphology and generation of ROS (Fig. 1). TNF expression is upregulated by *Pdk4*-deficiency, which can be attributed to the increased p65 nuclear translation and binding to the TNF promoter to activate it (Fig. 2). The activation of NF-κB-TNF pathway is responsible for shPDK4-induced apoptosis because knockdown of TNFR1 or p65 rescues cells from apoptotic death (Fig. 4). At the molecular level, we find that PDK4 binds to p65 under normal conditions and that ROS or glucose-depletion dissociates p65 from PDK4 protein, facilitating its release to the nucleus (Fig. 3). Using *in vivo* models, we show that *Pdk4*$^{-/-}$ liver is sensitized to liver injury with sustained JNK activation and GSH depletion. Overexpression of PDK4 prevents Jo2- and GalN/LPS-induced liver injury and apoptosis, which is associated with reduced hepatic ROS levels, p65 nuclear translocation, NF-κB activities and TNF production. In contrast, knockdown p65 or TNFR1 largely protects *Pdk4*$^{-/-}$ liver from undergoing apoptosis (Fig. 5 and Fig. 6). From these results, we conclude that the activation of NF-κB/TNF signaling promotes apoptosis under *Pdk4*-deficient conditions.

TNF can activate NF-κB to antagonize its death-inducing signaling. Our findings are not mutually exclusive with the previous notion that NF-κB activation is a survival mechanism that protects hepatocytes from TNF-mediated apoptosis by inducing pro-survival genes (35). We propose that NF-κB activation is not necessarily pro-survival, per se, but rather depends on the expression profile mediated by its activation. Further in-depth analyses show that the pro-survival activity of TNF is impaired, which is switched to a pro-apoptotic activity in *Pdk4*$^{-/-}$ hepatocytes (Fig. 7). These findings suggest that NF-κB activation is more than a simple on/off and is subjected to complex regulations. Sustained JNK activation (36, 37) and glutathione depletion (38, 39) may both contribute to TNF-induced apoptosis under *Pdk4*-deficient conditions. JNK activation amplifies ROS generation(40) and the latter further enhances JNK activity,(41) formatting a positive feedback loop to facilitate apoptotic death. The degree of protection by shTNFR1 against shPDK4-induced apoptosis is stronger than by shp65, suggesting that a direct blocking of TNF signal transduction is critical to prevent shPDK4-induced apoptosis.

TNF is a pleiotropic cytokine that is mainly produced by activated macrophages, but also by hepatocytes, albeit a small amount.(42) In shPDK4 HCC cells, the increased NF-κB/p65 nuclear translocation and subsequently the activation of TNF not only induce caspase-8, but also the intrinsic pathway initiator caspase-9. The latter is likely in part trigged by the increased cellular ROS production, an inducer of NF-κB and the intrinsic apoptosis pathway. (28) The numbers of aberrant mitochondria are significantly increased in shPDK4 cells, which may contribute to the sustained PDH activity and abnormal ROS production. Thus, ROS could be an intrinsic prerequisite for hepatic apoptosis triggered by loss of PDK4. It should be noted that GalN/LPS is a TNF-dependent model requiring NF-κB-dependent TNF production in liver non parenchymal cells (NPC) to induce apoptosis in GalN-sensitized hepatocytes. Therefore, our results do not exclude the involvement of NPC in PDK-mediated regulation of TNF production.

Intriguingly, the PDKs' pan-inhibitor dichloroacetate (DCA) and PDK4's specific inhibitor diisopropylamine dichloroacetate (DADA) exhibit anti-tumor efficacy in breast cancer models by inducing cell death.(43) In this regard, PDK4 inhibitors might be particularly useful in triggering cell death in HCC and other cancers.

Supplementary Material

Refer to Web version on PubMed Central for supplementary material.

Acknowledgments

We sincerely thank Dr. Robert A. Harris (Indiana University School of Medicine) for the *Pdk4*$^{-/-}$ mice, Dr. Maritza Abril and Dr. Xuanhao Sun at the Bioscience Electron Microscopy Laboratory of the University of Connecticut for the help with the transmission electron microscopy.

Grant Support

L.W. is supported by NIH ES025909, DK104656, AA024935, AA026322, VA Merit Award 1I01BX002634.

Abbreviations

Acetyl-CoA	acetyl-coenzyme A
ALT	Alanine Aminotransferase
BIRC2/3	baculoviral IAP repeat-containing 2/3
BCL2	B-cell lymphoma 2
CCDC103	coiled-coil domain containing 103
CD95	cluster of differentiation 95
CHIP-qPCR	chromatin immunoprecipitation-quantitative PCR
CHX	cycloheximide
c-IAP1/2	cellular inhibitor of apoptosis protein 1/2
Co-IP	co-immunoprecipitation
DADA	diisopropylamine dichloroacetate
DCA	dichloroacetate
DISC	death-inducing signaling complex
ECAR	extracellular acidification rate
ELISA	enzyme-linked immunosorbent assay
GalN	D-(+)-Galactosamine
GSH	Glutathione
GST	glutathione S-transferase

HCC	hepatocellular carcinoma
IL-1β	interleukin-1 beta
IL-1R	interleukin-1 receptor
JNK	c-Jun N-terminal Kinase
LPS	Lipopolysaccharide
NAD/NADH	nicotinamide adenine dinucleotide
NF-κB	nuclear factor kappa-light-chain-enhancer of activated B cells
OCR	oxygen consumption rate
PARP	poly (ADP-ribose) polymerase
PDC	pyruvate dehydrogenase complex
PDH	pyruvate dehydrogenase
PDK4	pyruvate dehydrogenase kinase 4
ROS	reactive oxygen species
shCon	control shRNA
shCTL	control shRNA
shRNA	small hairpin RNA
SMAD1/5/8	mothers against decapentaplegic homolog 1/5/8
TCA cycle	the tricarboxylic acid cycle
TEM	transmission electron microscopy
TNF	tumor necrosis factor
TNFR1/2	tumor necrosis factor receptor 1/2
TRAF2	TNFR-associated factor 2
TUNEL	terminal deoxynucleotidyl transferase dUTP nick end labeling
WT	wide type

References

1. Behal RH, Buxton DB, Robertson JG, Olson MS. Regulation of the pyruvate dehydrogenase multienzyme complex. Annu Rev Nutr. 1993; 13:497–520. [PubMed: 8369156]

2. Jeoung NH, Harris RA. Pyruvate dehydrogenase kinase-4 deficiency lowers blood glucose and improves glucose tolerance in diet-induced obese mice. Am J Physiol Endocrinol Metab. 2008; 295:E46–54. [PubMed: 18430968]

3. Liu Z, Chen X, Wang Y, Peng H, Wang Y, Jing Y, Zhang H. PDK4 protein promotes tumorigenesis through activation of cAMP-response element-binding protein (CREB)-Ras homolog enriched in brain (RHEB)-mTORC1 signaling cascade. J Biol Chem. 2014; 289:29739–29749. [PubMed: 25164809]

4. Lee SJ, Jeong JY, Oh CJ, Park S, Kim JY, Kim HJ, Doo Kim N, et al. Pyruvate Dehydrogenase Kinase 4 Promotes Vascular Calcification via SMAD1/5/8 Phosphorylation. Sci Rep. 2015; 5:16577. [PubMed: 26560812]

5. Zhang Y, Soto J, Park K, Viswanath G, Kuwada S, Abel ED, Wang L. Nuclear receptor SHP, a death receptor that targets mitochondria, induces apoptosis and inhibits tumor growth. Mol Cell Biol. 2010; 30:1341–1356. [PubMed: 20065042]

6. Chu WM. Tumor necrosis factor. Cancer Lett. 2013; 328:222–225. [PubMed: 23085193]

7. Hoesel B, Schmid JA. The complexity of NF-kappaB signaling in inflammation and cancer. Mol Cancer. 2013; 12:86. [PubMed: 23915189]

8. Luedde T, Schwabe RF. NF-kappaB in the liver--linking injury, fibrosis and hepatocellular carcinoma. Nat Rev Gastroenterol Hepatol. 2011; 8:108–118. [PubMed: 21293511]

9. Yamada Y, Kirillova I, Peschon JJ, Fausto N. Initiation of liver growth by tumor necrosis factor: deficient liver regeneration in mice lacking type I tumor necrosis factor receptor. Proc Natl Acad Sci U S A. 1997; 94:1441–1446. [PubMed: 9037072]

10. Czaja MJ, Xu J, Alt E. Prevention of carbon tetrachloride-induced rat liver injury by soluble tumor necrosis factor receptor. Gastroenterology. 1995; 108:1849–1854. [PubMed: 7768392]

11. Xu Y, Bialik S, Jones BE, Iimuro Y, Kitsis RN, Srinivasan A, Brenner DA, et al. NF-kappaB inactivation converts a hepatocyte cell line TNF-alpha response from proliferation to apoptosis. Am J Physiol. 1998; 275:C1058–1066. [PubMed: 9755059]

12. He G, Karin M. NF-kappaB and STAT3 - key players in liver inflammation and cancer. Cell Res. 2011; 21:159–168. [PubMed: 21187858]

13. Choiniere J, Wu J, Wang L. Pyruvate Dehydrogenase Kinase 4 Deficiency Results in Expedited Cellular Proliferation through E2F1-Mediated Increase of Cyclins. Mol Pharmacol. 2017; 91:189–196. [PubMed: 28003426]

14. Chen X, Ding WX, Ni HM, Gao W, Shi YH, Gambotto AA, Fan J, et al. Bid-independent mitochondrial activation in tumor necrosis factor alpha-induced apoptosis and liver injury. Mol Cell Biol. 2007; 27:541–553. [PubMed: 17101783]

15. Zhang Y, Liu C, Barbier O, Smalling R, Tsuchiya H, Lee S, Delker D, et al. Bcl2 is a critical regulator of bile acid homeostasis by dictating Shp and lncRNA H19 function. Sci Rep. 2016; 6:20559. [PubMed: 26838806]

16. Zhang Y, Xu N, Xu J, Kong B, Copple B, Guo GL, Wang L. E2F1 is a novel fibrogenic gene that regulates cholestatic liver fibrosis through the Egr-1/SHP/EID1 network. Hepatology. 2014; 60:919–930. [PubMed: 24619556]

17. Song Y, Liu C, Liu X, Trottier J, Beaudoin M, Zhang L, Pope C, et al. H19 promotes cholestatic liver fibrosis by preventing ZEB1-mediated inhibition of epithelial cell adhesion molecule. Hepatology. 2017; 66:1183–1196. [PubMed: 28407375]

18. Liu C, Yang Z, Wu J, Zhang L, Lee S, Shin DJ, Tran M, et al. lncRNA H19 interacts with polypyrimidine tract-binding protein 1 to reprogram hepatic lipid homeostasis. Hepatology. 2017

19. Smalling RL, Delker DA, Zhang Y, Nieto N, McGuiness MS, Liu S, Friedman SL, et al. Genome-wide transcriptome analysis identifies novel gene signatures implicated in human chronic liver disease. Am J Physiol Gastrointest Liver Physiol. 2013; 305:G364–374. [PubMed: 23812039]

20. Tsuchiya H, da Costa KA, Lee S, Renga B, Jaeschke H, Yang Z, Orena SJ, et al. Interactions Between Nuclear Receptor SHP and FOXA1 Maintain Oscillatory Homocysteine Homeostasis in Mice. Gastroenterology. 2015; 148:1012–1023. e1014. [PubMed: 25701738]

21. Vikis HG, Guan KL. Glutathione-S-transferase-fusion based assays for studying protein-protein interactions. Methods Mol Biol. 2004; 261:175–186. [PubMed: 15064458]

22. Datta S, Wang L, Moore DD, Osborne TF. Regulation of 3-hydroxy-3-methylglutaryl coenzyme A reductase promoter by nuclear receptors liver receptor homologue-1 and small heterodimer partner: a mechanism for differential regulation of cholesterol synthesis and uptake. J Biol Chem. 2006; 281:807–812. [PubMed: 16282330]
23. Zhao Y, Yang Z, Wu J, Wu R, Keshipeddy SK, Wright D, Wang L. High-mobility-group protein 2 regulated by microRNA-127 and small heterodimer partner modulates pluripotency of mouse embryonic stem cells and liver tumor initiating cells. Hepatol Commun. 2017; 1:816–830. [PubMed: 29218329]
24. Yang Z, Tsuchiya H, Zhang Y, Lee S, Liu C, Huang Y, Vargas GM, et al. REV-ERBalpha Activates C/EBP Homologous Protein to Control Small Heterodimer Partner-Mediated Oscillation of Alcoholic Fatty Liver. Am J Pathol. 2016; 186:2909–2920. [PubMed: 27664470]
25. Zhang L, Yang Z, Trottier J, Barbier O, Wang L. Long noncoding RNA MEG3 induces cholestatic liver injury by interaction with PTBP1 to facilitate shp mRNA decay. Hepatology. 2017; 65:604–615. [PubMed: 27770549]
26. Zhou T, Zhang Y, Macchiarulo A, Yang Z, Cellanetti M, Coto E, Xu P, et al. Novel polymorphisms of nuclear receptor SHP associated with functional and structural changes. J Biol Chem. 2010; 285:24871–24881. [PubMed: 20516075]
27. Barkett M, Gilmore TD. Control of apoptosis by Rel/NF-kappaB transcription factors. Oncogene. 1999; 18:6910–6924. [PubMed: 10602466]
28. Gloire G, Legrand-Poels S, Piette J. NF-kappaB activation by reactive oxygen species: fifteen years later. Biochem Pharmacol. 2006; 72:1493–1505. [PubMed: 16723122]
29. Liboni KC, Li N, Scumpia PO, Neu J. Glutamine modulates LPS-induced IL-8 production through IkappaB/NF-kappaB in human fetal and adult intestinal epithelium. J Nutr. 2005; 135:245–251. [PubMed: 15671221]
30. Saleem M, Qadir MI, Perveen N, Ahmad B, Saleem U, Irshad T. Inhibitors of apoptotic proteins: new targets for anticancer therapy. Chem Biol Drug Des. 2013; 82:243–251. [PubMed: 23790005]
31. Panizzi JR, Becker-Heck A, Castleman VH, Al-Mutairi DA, Liu Y, Loges NT, Pathak N, et al. CCDC103 mutations cause primary ciliary dyskinesia by disrupting assembly of ciliary dynein arms. Nat Genet. 2012; 44:714–719. [PubMed: 22581229]
32. Brenner D, Blaser H, Mak TW. Regulation of tumour necrosis factor signalling: live or let die. Nat Rev Immunol. 2015; 15:362–374. [PubMed: 26008591]
33. Ogasawara J, Watanabe-Fukunaga R, Adachi M, Matsuzawa A, Kasugai T, Kitamura Y, Itoh N, et al. Lethal effect of the anti-Fas antibody in mice. Nature. 1993; 364:806–809. [PubMed: 7689176]
34. Morgan MJ, Liu ZG. Crosstalk of reactive oxygen species and NF-kappaB signaling. Cell Res. 2011; 21:103–115. [PubMed: 21187859]
35. Ding WX, Yin XM. Dissection of the multiple mechanisms of TNF-alpha-induced apoptosis in liver injury. J Cell Mol Med. 2004; 8:445–454. [PubMed: 15601573]
36. Liu H, Lo CR, Czaja MJ. NF-kappaB inhibition sensitizes hepatocytes to TNF-induced apoptosis through a sustained activation of JNK and c-Jun. Hepatology. 2002; 35:772–778. [PubMed: 11915022]
37. Schwabe RF, Uchinami H, Qian T, Bennett BL, Lemasters JJ, Brenner DA. Differential requirement for c-Jun NH2-terminal kinase in TNFalpha- and Fas-mediated apoptosis in hepatocytes. FASEB J. 2004; 18:720–722. [PubMed: 14766793]
38. Nagai H, Matsumaru K, Feng G, Kaplowitz N. Reduced glutathione depletion causes necrosis and sensitization to tumor necrosis factor-alpha-induced apoptosis in cultured mouse hepatocytes. Hepatology. 2002; 36:55–64. [PubMed: 12085349]
39. Matsumaru K, Ji C, Kaplowitz N. Mechanisms for sensitization to TNF-induced apoptosis by acute glutathione depletion in murine hepatocytes. Hepatology. 2003; 37:1425–1434. [PubMed: 12774022]
40. Chambers JW, LoGrasso PV. Mitochondrial c-Jun N-terminal kinase (JNK) signaling initiates physiological changes resulting in amplification of reactive oxygen species generation. J Biol Chem. 2011; 286:16052–16062. [PubMed: 21454558]

41. Kamata H, Honda S, Maeda S, Chang L, Hirata H, Karin M. Reactive oxygen species promote TNFalpha-induced death and sustained JNK activation by inhibiting MAP kinase phosphatases. Cell. 2005; 120:649–661. [PubMed: 15766528]

42. Spencer NY, Zhou W, Li Q, Zhang Y, Luo M, Yan Z, Lynch TJ, et al. Hepatocytes produce TNF-alpha following hypoxia-reoxygenation and liver ischemia-reperfusion in a NADPH oxidase- and c-Src-dependent manner. Am J Physiol Gastrointest Liver Physiol. 2013; 305:G84–94. [PubMed: 23639811]

43. Su L, Zhang H, Yan C, Chen A, Meng G, Wei J, Yu D, et al. Superior anti-tumor efficacy of diisopropylamine dichloroacetate compared with dichloroacetate in a subcutaneous transplantation breast tumor model. Oncotarget. 2016

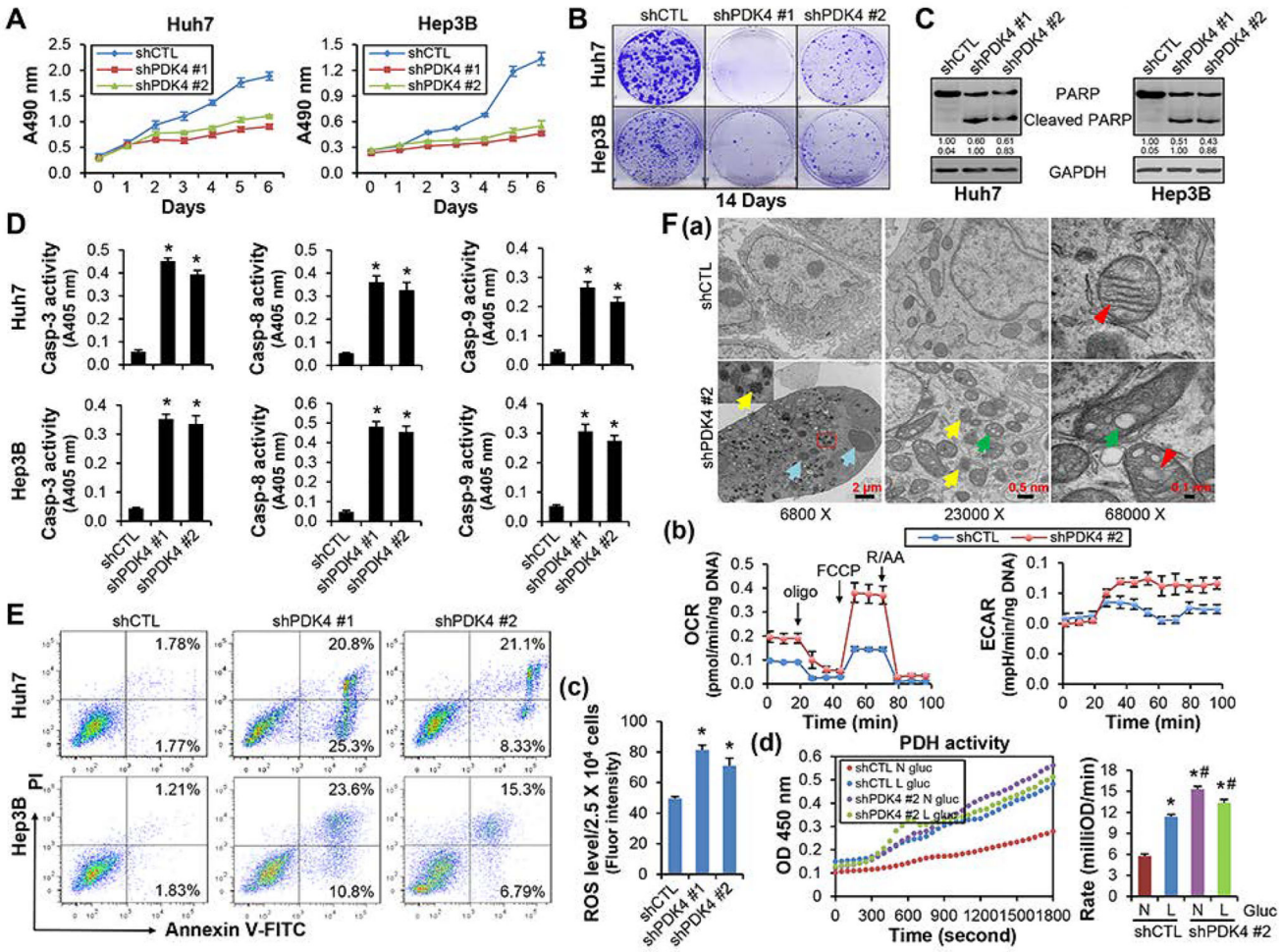

Figure 1.

Knockdown of PDK4 in HCC cells induced apoptotic cell death and increased abnormal mitochondrial numbers and ROS production. (A) MTS assay to determine cell viability in control (shCTL) and PDK4 knockdown (shPDK4) Huh7 (left) and Hep3B (right) cells. (B) Colony formation assay for 14 days in shCTL and shPDK4 Huh7 and Hep3B cells. (C) WB of PARP protein. (D) Caspase-3, -8 and -9 activities were measured using a colorimetric method. (E) Flow cytometry using Annexin V and PI staining to determine the apoptosis rate. (F-a) Transmission electron microscopy (TEM) of mitochondria morphology in shCTL and shPDK4 Huh7 cells at day 10 after shRNA transfection. Blue arrow: condensed chromatin; yellow arrow: abnormal mitochondria; green arrow: mitochondria vacuolization; red arrowhead: normal (shCTL) or swollen and distorted (shPDK4) mitochondria cristae. A minimum of 10 cells per condition were examined. (F-b) Seahorse analysis in shCTL and shPDK4 Huh7 cells. Oxygen consumption rate (OCR) and extracellular acidification rate (ECAR) were monitored following the sequential addition of oligomycin (an inhibitor of ATP synthase), FCCP (uncoupling electron transport from ATP generation in the inner Mitochondria membrane) and rotenone/antimycin A (R/AA, inhibiting mitochondria complex I and III respectively) using the 24-well Seahorse XFe24 Extracellular Analyzer. Individual wells were normalized using the amount of DNA (ng). (F-c) ROS levels in shCTL

and shPDK4 Huh7 cells. (F-d) PDH activities in shCTL and shPDK4 Huh7 cells. Cells were cultured in DMEM medium containing either normal (N, 4.5 g/L) or low (L, 1.0 g/L) glucose for 48 hr. D, F-c: Data are shown as mean ± SEM of three independent experiments with triplicate assays. *$P < .01$ vs shCTL. F-d: Data are shown as mean ± SEM. *$P < .01$ vs N-shCTL; $^{\#}P < .01$ vs L-shCTL.

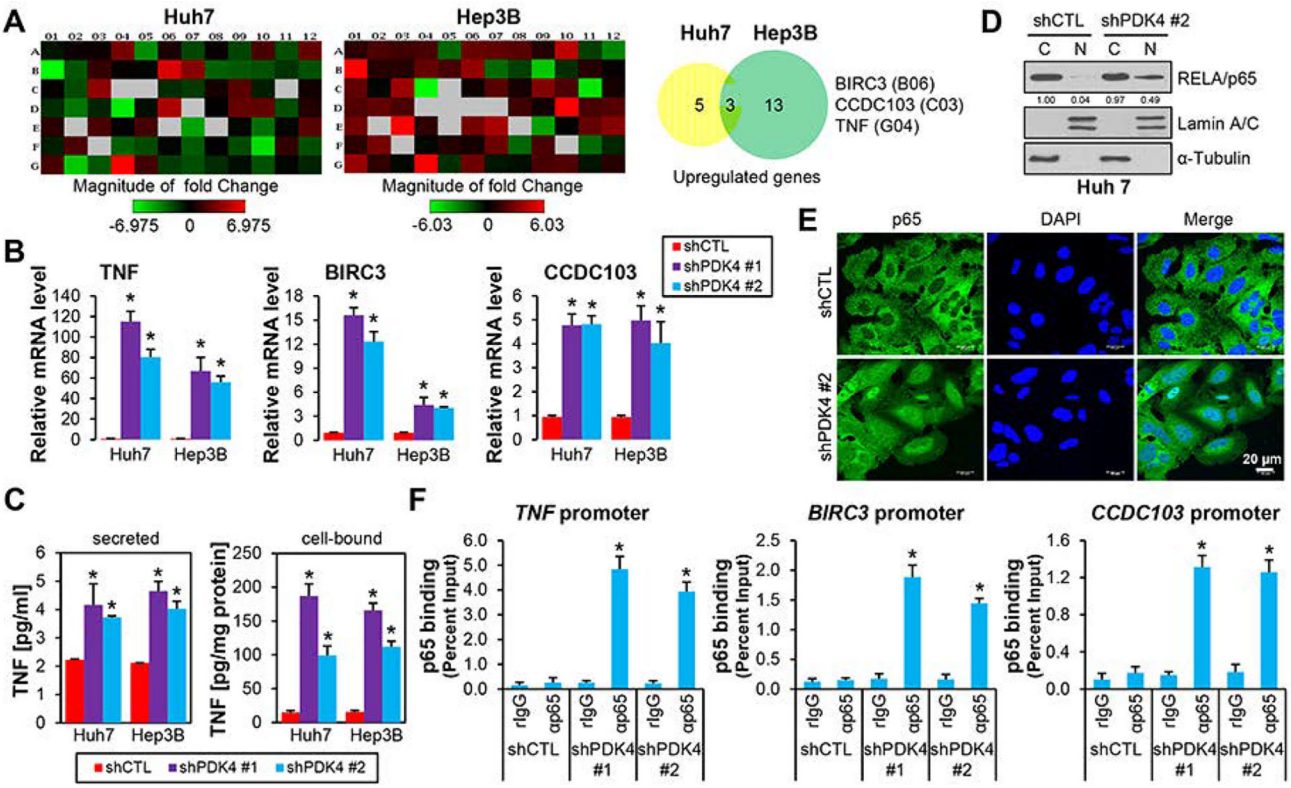

Figure 2.

PDK4-deficiency induced p65 nuclear translocation and its activation of TNF expression. (A) PCR array profile. Total RNAs from shCTL and shPDK4 Huh7 and Hep3B cell were extracted and subjected to Human Cell Death PathwayFinder PCR Array analysis. The fold changes of individual genes were represented in heat map (left) and the upregulated genes (fold > 2.0) were shown in pie charts (right). (B) qPCR of *TNF, BIRC3* and *CCDC103* mRNAs in shCTL and shPDK4 Huh7 and Hep3B cells. (C) ELISA assay of secreted or cellular TNF proteins in shCTL and shPDK4 Huh7 and Hep3B cells. (D) WB of cytoplasmic (C) and nuclear (N) NF-κB/p65 proteins in shCTL and shPDK4 Huh7 cells. Lamin A/C, nuclear marker; α-tubulin, cytoplasmic marker. (E) Immunofluorescence of nuclear and cytoplasmic localization of NF-κB/p65 in shCTL and shPDK4 Huh7 cells. Nucleus was counter-stained with DAPI. (F) ChIP assays of NF-κB/p65 occupancy on *TNF, BIRC3* and *CCDC103* promoters in shCTL and shPDK4 Huh7 cells. B, C, F: Data are shown as mean ± SEM of three independent experiments with triplicate assays. **P* < .01 vs shCTL.

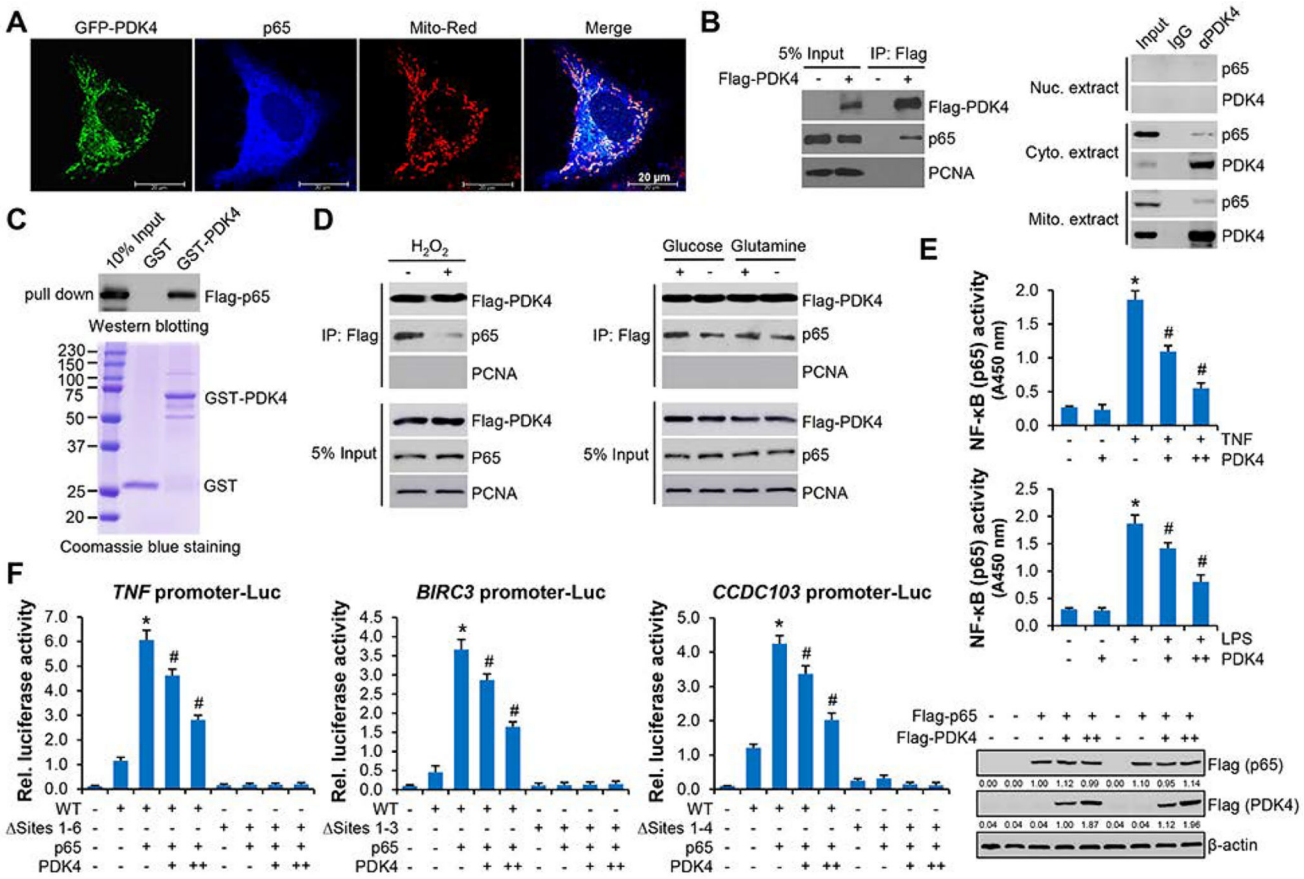

Figure 3.

PDK4 sequestrated p65 protein in cytosol via protein-protein interaction. (A) Confocal microscopy in Huh7 cells. PDK4 protein was detected by GFP and p65 protein was detected by p65 antibody. (B) Left: Co-IP in Huh7 cells transfected with empty vector (−) or Flag-PDK4 (+) plasmids. The immunoprecipitated complex was resolved by Western blot with Flag (PDK4) or p65 antibodies, respectively. Right: Co-IP to detect the endogenous interaction between PDK4 and p65 in nuclear (Nuc.), cytosolic (Cyto.) and mitochondrial (Mito.) extracts from Hepa1 cells using PDK4 antibody. (C) GST pull-down assays with GST or GST-PDK4 purified from *E. coli* and *in vitro* transcribed/translated p65 (top). The expression of GST and GST-PDK4 were examined with Coomassie blue staining (bottom). (D) Co-IP followed by WB in Huh7 cells transfected with Flag-PDK4. Left: cells were treated with (+) or without (−) 200 μM H_2O_2 for 6 hr. Right: cells were cultured in medium with (+) or without (−) glucose or glutamine for 48 hr. (E) Nuclear p65 activities in Huh7 cells transfected with empty vector or Flag-PDK4 in the presence or absence of TNF (10 ng/ml) or LPS (10 ng/ml) for 30 min. Data are shown as mean ± SEM. $^{*}P < .01$ vs (−); $^{\#}P < .01$ PDK4 + TNF or LPS vs TNF or LPS alone. (F) Left: Luciferase reporter assays. *TNF, BIRC3* and *CCDC103* promoter reporters or their mutant reporters were transfected with p65 expression plasmids in combination with PDK4 (+, 200 ng; ++, 400 ng). Data are shown are mean ± SEM. $^{*}P < .01$ vs mock (−); $^{\#}P < .01$ PDK4 vs p65 (+). Right: WB of p65 and PDK4 proteins.

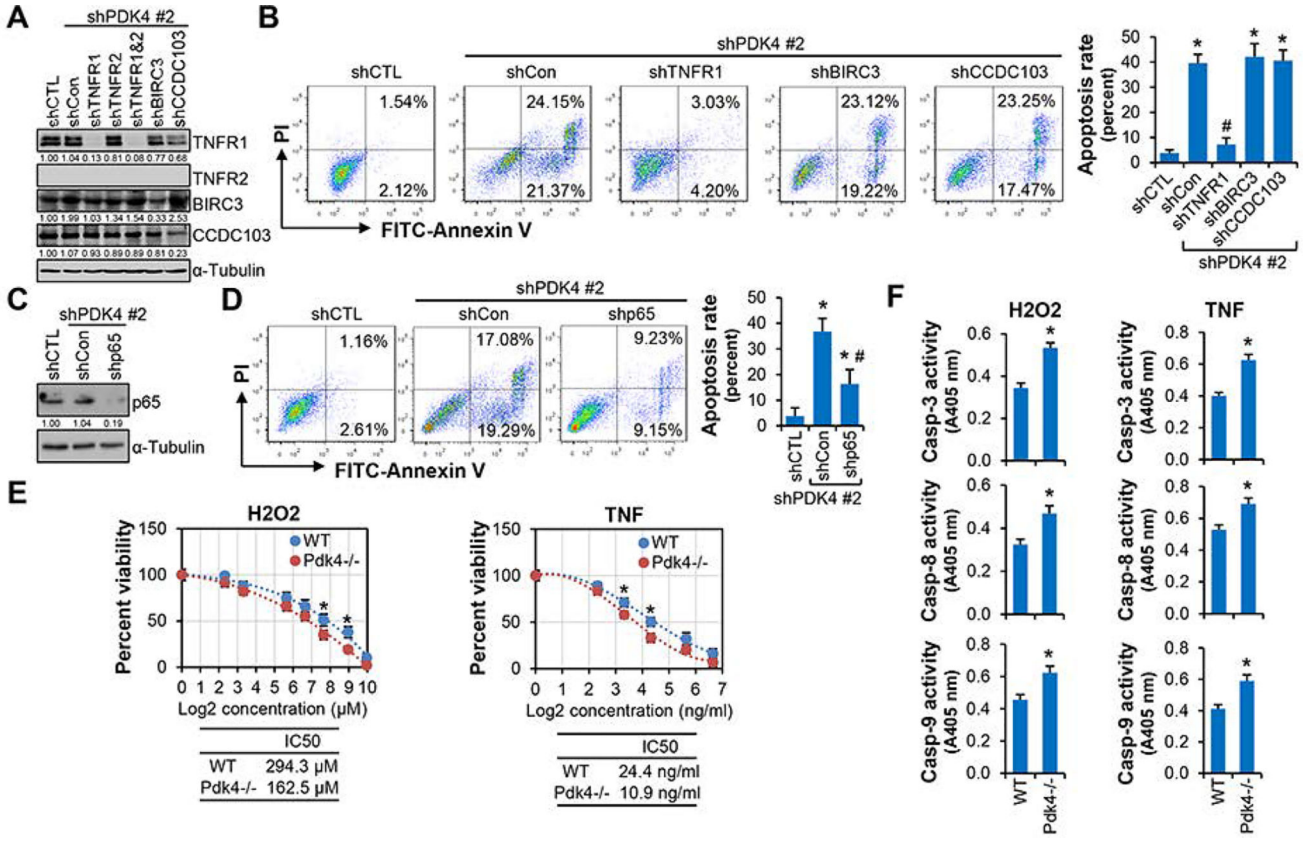

Figure 4.

Inhibition of NF-κB/TNF signaling impaired PDK4-mediated apoptosis. (A) Western blot. shPDK4 Huh7 cells were transduced with lentiviral control (shCon) or shRNAs targeting TNFR1, TNFR2, BIRC3, or CCDC103, respectively, and whole cell lysates were used. (B) Flow cytometry using Annexin V and PI staining. The bar graph (right) represented statistics of total (early and late) apoptotic cells. $^{*}P < .01$ vs shCTL; $^{\#}P < .01$ vs shCon. (C) Western blot of p65 protein expression. (D) Flow cytometry using Annexin V and PI staining. (E) MTS assay to determine cell viability. Primary hepatocytes from WT and *Pdk4*$^{-/-}$ mice were treated with H2O2 or TNF for 24 hr. Data were plotted as percent viability versus log2 transformed concentrations. $^{*}P < .01$ WT vs *Pdk4*$^{-/-}$. (F) Caspase-3, -8 and -9 activities in WT and *Pdk4*$^{-/-}$ primary hepatocytes treated with H2O2 (300 μM) or TNF (25 ng/ml) for 24 hr. Data are shown as mean ± SEM. $^{*}P < .01$ vs WT. E, F: 10 μg/ml cycloheximide was used to sensitize the apoptosis-inducing effect of TNF.

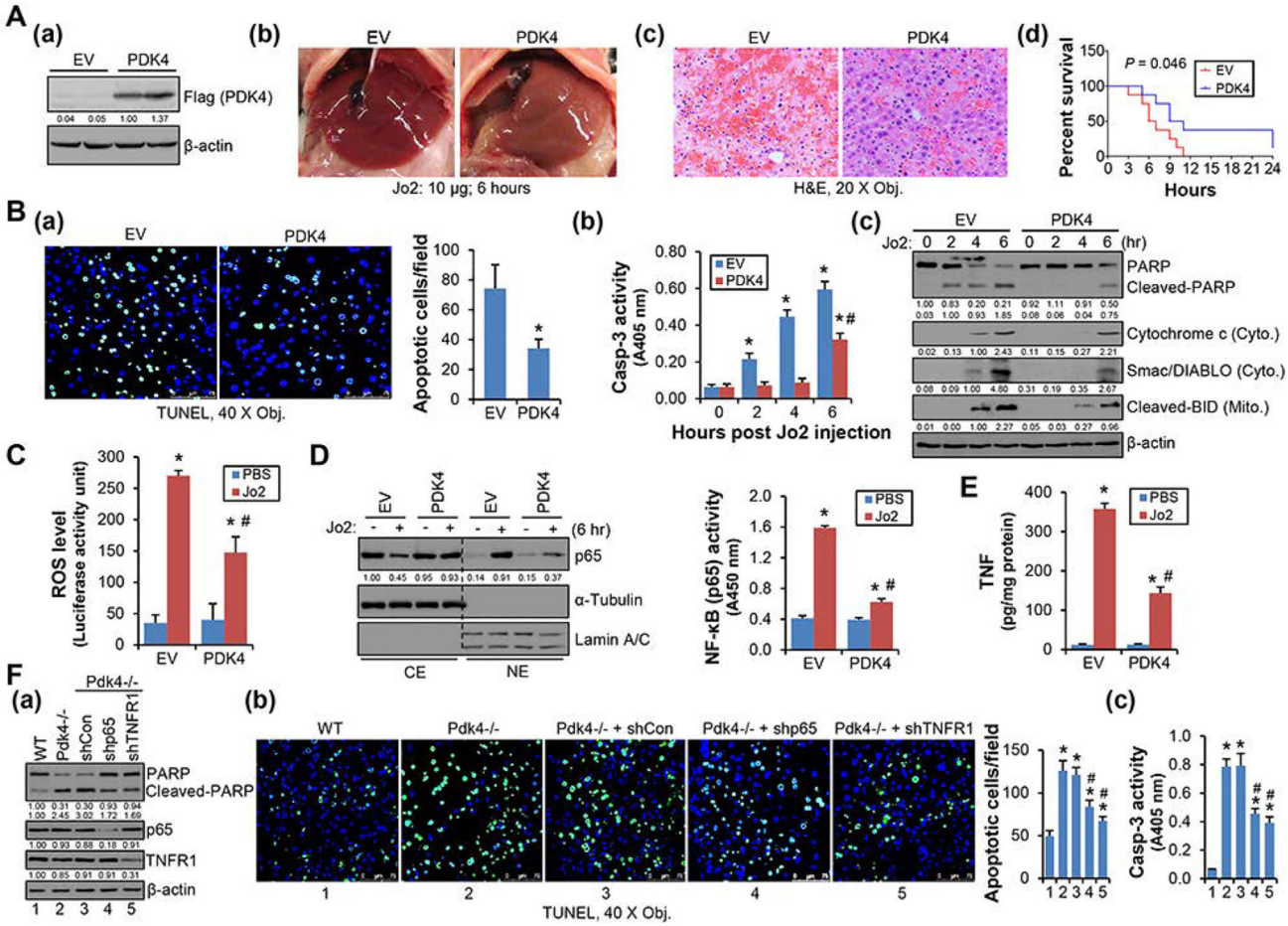

Figure 5.

Overexpression of PDK4 alleviated Jo2-induced hepatic apoptosis. (A-a) WB of PDK4 protein in liver tissue lysates from 8-week-old WT mice 72 hr after transfection with empty vector (EV) or Flag-tagged PDK4 (PDK4). (A-b, A-c) Gross liver morphology (A-b) and H&E staining of liver sections (A-c). Jo2: 6 hr, 10 μg/mouse. (A-d) Lethal effect of Jo2 in mice. The percentages of mice surviving until the indicated time were plotted (n = 20). (B-a) TUNEL staining of liver sections. Jo2: 6 hr. The histogram represented statistical analysis of 20 fields. *$P < .01$ vs EV. (B-b, B-c) Caspase-3 activity (B-b) and WB of PARP and BID cleavage, Cytochrome C and Smac/DIABLO release (B-c) in liver tissue lysates. Cyto., cytosolic fraction; Mito., mitochondrial fraction. *$P < .01$ vs 0 hr; $^{\#}P < .01$ vs 6 hr-EV. (C) ROS activity was determined using L-012. The luminescence was measured in liver tissue lysates (Jo2: 6 hr). (D) Left: WB of p65 protein in cytoplasmic extract (CE) and nuclear extract (NE) prepared from liver tissues. Right: Measurement of liver NF-κB (p65) activity with nuclear extracts. (E) ELISA of TNF expression in the liver tissues. Jo2: 6 hr. (F) Knockdown of p65 and TNFR1 alleviated Jo2-induced apoptosis in *Pdk4*$^{-/-}$ livers. WB of PARP cleavage (F-a), TUNEL staining of liver sections (F-b), and caspase-3 activity in liver tissue lysates (F-c). Eight-week-old *Pdk4*$^{-/-}$ mice were injected with control (shCon), shp65, or shTNFR1 plasmids via tail vein. Three days after transfection, mice were injected with Jo2 (5 μg/mouse) and livers were collected 6 hr later. B-F: Each group represents a pooled

sample (equal amounts of protein) from 5 individual mice with triplicate assays. Data are shown as mean ± SEM. C, D, E: *$P < .01$ vs EV-PBS; $^{\#}P < .01$, PDK4-Jo2 vs EV-Jo2. F: *$P < .01$ vs WT; $^{\#}P < .01$ vs *Pdk4*$^{-/-}$ + shCon.

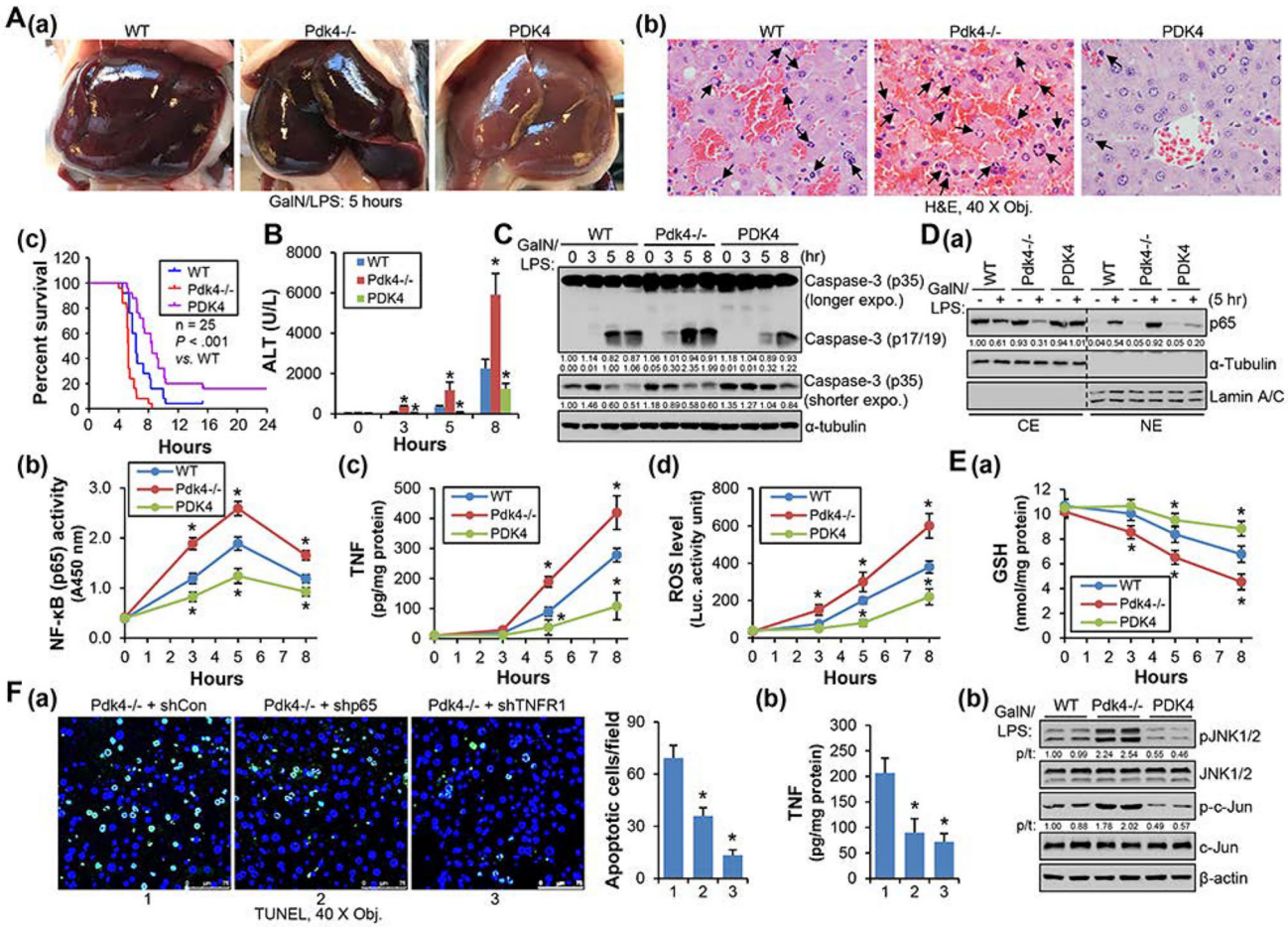

Figure 6.

Overexpression of PDK4 prevented GalN/LPS-induced hepatic apoptosis. (A-a, -b) Gross liver morphology (A-a) and H&E staining of liver sections (A-b) of 8-week-old WT, *Pdk4*$^{-/-}$ and PDK4-overexpressed (PDK4) mice 5 hr after GalN/LPS injection. (A-c) Lethal effect of GalN/LPS in mice. The percentages of mice survival at the indicated time were plotted (n = 25). (B) Plasma ALT levels in GalN/LPS treated mice. (C) WB of caspase-3 in liver tissue lysates. (D-a) WB of p65 protein in cytoplasmic extract (CE) and nuclear extract (NE) prepared from liver tissues. (D-b) Measurement of liver NF-κB (p65) activity in nuclear extracts. (D-c, -d) ELISA of TNF expression and ROS activity in liver tissues collected at different time point. (E-a) GSH levels were determined in liver tissues collected at different time point. (E-b) WB of JNK and c-Jun phosphorylation. The ratio of phosphorylation vs total form (p/t) was densitometrically quantitated and denoted. (F-a) TUNEL staining of liver sections. 8-week-old *Pdk4*$^{-/-}$ mice were injected with control (shCon), shp65, or shTNFR1 plasmids via tail vein. Three days later, mice were injected with GalN/LPS and livers were collected 5 hr later. The histogram represented statistical analysis of apoptotic cells of 20 fields. (E-b) ELISA of hepatic TNF in the livers described in (E-a). All data are shown as mean ± SEM. B, D-b, D-c, D-d, E-a: **P* < .01 vs WT. F-a, -b: **P* < .01 vs *Pdk4*$^{-/-}$ + shCon.

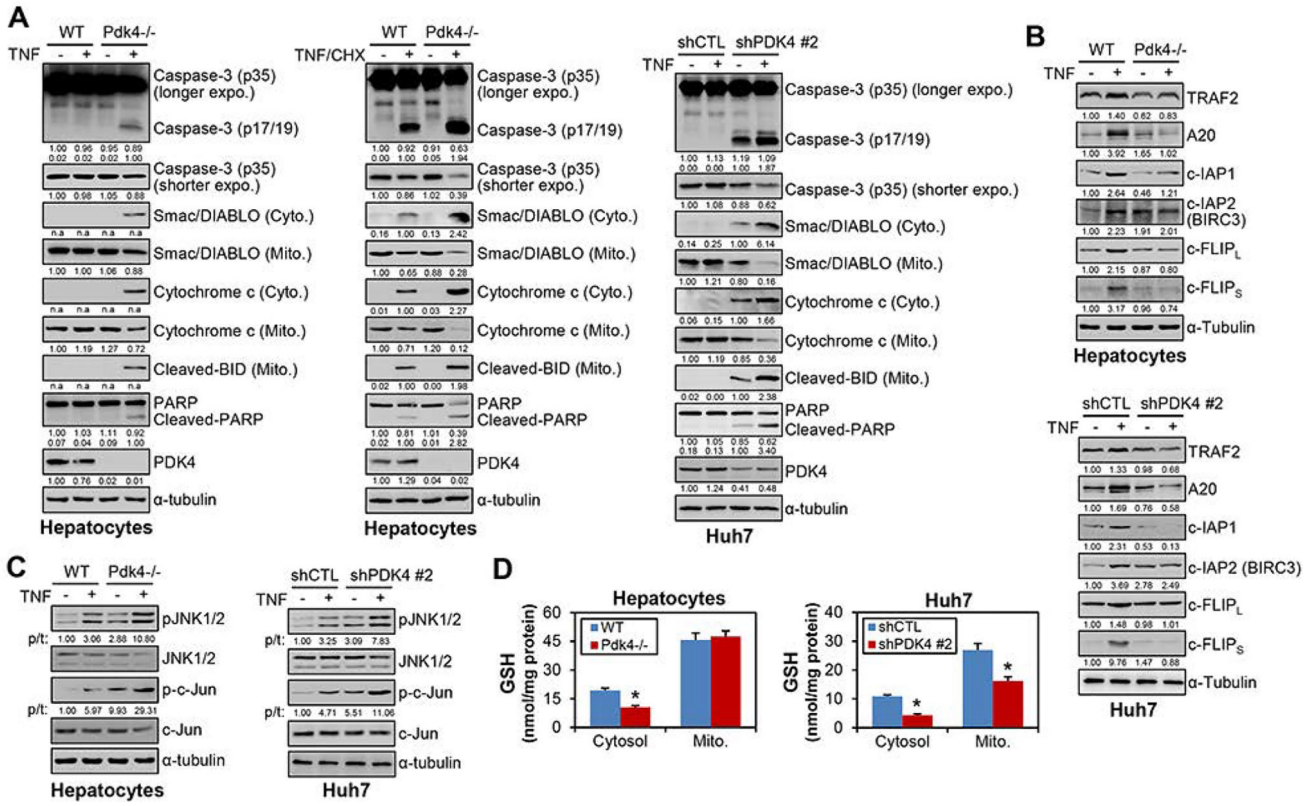

Figure 7.

PDK4-deficiency impaired the pro-survival function of NF-κB. (A) Primary hepatocytes from WT and *Pdk4*$^{-/-}$ mice and Huh7 cells were treated with TNF (20 ng/ml) or TNF + cycloheximide (CHX, 10 μg/ml) for 24 hr. Whole cell lysates, cytosolic (Cyto.) and mitochondrial (Mito.) fractions were prepared and subjected to WB with the indicated antibodies. n.a.: non-applicable for densitometric quantification as no bands in other groups for comparison.

(B) WT and *Pdk4*$^{-/-}$ hepatocytes and Huh7 cells were treated with TNF (20 ng/ml) for 24 hr. Whole cell lysates were prepared and subjected to WB with the indicated antibodies against pro-survival proteins. (C) WB was performed to examine JNK and c-Jun phosphorylation in whole cell lysates of hepatocytes and Huh7 cells treated with TNF (20 ng/ml) for 1 hr. The ratio of phosphorylation vs total form (p/t) was densitometrically quantitated and denoted. (D) The cytosol and mitochondrion (Mito.) fractions were prepared from WT and *Pdk4*$^{-/-}$ hepatocytes, or shCTL and shPDK4 Huh7 cells, and the reduced glutathione (GSH) was determined. **P* < .05 vs WT or shCTL.

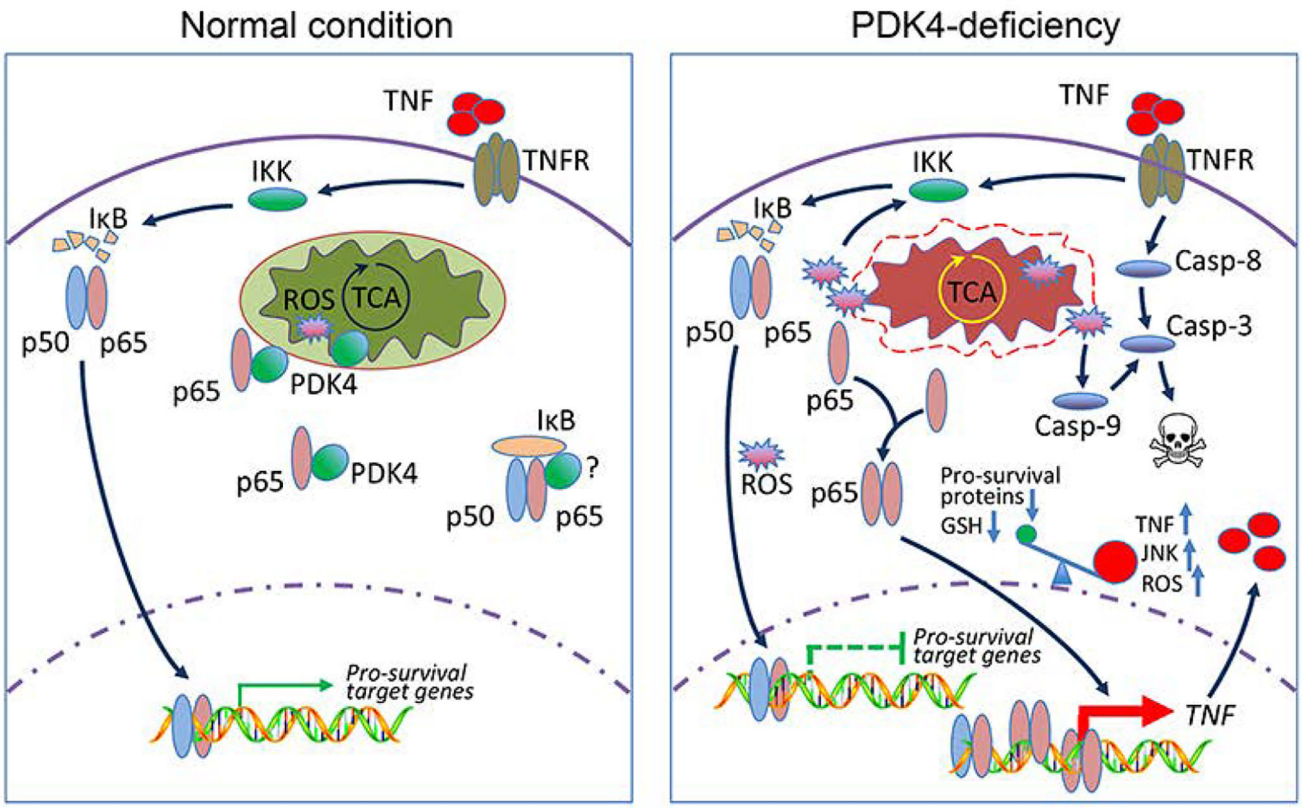

Figure 8.

Schematic showing PDK4 as a checkpoint in NF-κB/TNF-mediated apoptosis. Under normal cellular conditions, PDK4 interacts with NF-κB/p65 and sequesters p65 in the cytoplasm. Mitochondria respiration and ROS production remain normal. TNF treatment can activate NF-κB (p50/p65 complex) signaling to promote the induction of pro-survival genes. Knockdown of PDK4 disrupts mitochondria respiration and generates excessive ROS; the latter facilitates PDK4 and p65 protein dissociation, and releases p65 to accelerate its nuclear translocation. Excessive ROS may also deplete cellular GSH and activate JNK. In this scenario, in the nucleus of PDK4-deficient cells, pro-survival genes are less/not responsive to p65 transactivation, whereas TNF is activated which in turn induces caspase-8 and the extrinsic apoptosis pathway. In addition, ROS leads to activation of caspase-9 and the intrinsic apoptosis pathway. Collectively, we propose that increased ROS, decreased GSH, and sustained JNK activation shift the pro-survival function NF-κB toward facilitating TNF-mediated apoptosis.